



Journal of Advanced Research in Fluid Mechanics and Thermal Sciences

Journal homepage:
https://semarakilmu.com.my/journals/index.php/fluid_mechanics_thermal_sciences/index
ISSN: 2289-7879



Effect of Chemical Reaction and Variable Thermal Conductivity in MHD Williamson Nanofluid Flow with Gyrotactic Microorganisms

Poludasu Madhu Sravanthi¹, Maddali Radha Madhavi^{1,*}, Sridhar Wuriti¹

¹ Department of Engineering Mathematics, College of Engineering, Koneru Lakshmaiah Education Foundation, Guntur, AP, 520002, India

ARTICLE INFO

Article history:

Received 18 September 2023

Received in revised form 10 December 2023

Accepted 24 December 2023

Available online 15 January 2024

Keywords:

Gyrotactic microorganisms; MHD; chemical reaction; thermal conductivity; Peclet number

ABSTRACT

The primary objective of this study deals with numerical analysis of gyrotactic microorganisms in Williamson nanofluids under the influence of chemical reaction and variable thermal conductivity along with porous medium. Using the similarity transformations, the non-linear PDEs are transformed into ODEs. RK-Fehlberg with a shooting strategy utilised to address ODEs with the influence of MATLAB software. Effect of Permeability, Prandtl number, magnetic field, Williamson parameter, Schmidt number, Peclet number, the profiles of velocity, temperature, concentration, and motile microbe density are explored in detail, and the potential results are displayed in graphs. The density number, Nusselt number, skin friction coefficient, and Sherwood number displayed in tables.

1. Introduction

Recently researchers studied promoting on the temperature suspension (inferior to 100 nm in size) of immaculate liquids i.e., water, oils and other nanofluids. In fresh water these nanoparticles that is metallic copper, silver, etc., carry out and manage the transfer of heat, the kind of heat carrier and heat exchangers depends critically on these liquids. Choi and Eastman [1] proposed as non-Newtonian flows are developed and used, nanoparticles are employed to boost thermal conductivity of fluids. Khan *et al.*, [2] explored the structure of nanofluids in many contexts and forms. The second rule of thermodynamics is used to study how entropy increases and decreases when temperature radiation interacts with nanofluids moving via slender ends.

Nield and Kuznetsov [3] developed Buongiorno work. Both authors use Thermophoretic and Brownian terms went to electrical equations to investigate how Brownian movement and thermophoresis affect these equations by putting forth a number of fresh, potentially problematic scenarios. A vast number of nanoparticles were used to study biological convection [4,5]. Mallikarjuna *et al.*, [6] studied continuous biomarkers of nanofluids and contracted microbes in a vertical kiln, dimensionless variation to convert integrating experimental issues into non-intrusive

* Corresponding author.

E-mail address: mrmadhavi5@gmail.com

<https://doi.org/10.37934/arfmts.113.1.6781>

models, and the distinction a comparison of finite and numerical numbers. A mathematical framework was provided to analyse the impact of secondary velocity slides on horizontal filter plates [7]. Shahid *et al.*, [8] developed the paper provides a numerical assessment of water-based nanofluid flow with MHD, heat, and mass transfer across a porous permeable shrinking/stretching sheet of gyrotactic bacteria in motion. In the current study, the effect of the magnetic field, heat radiation, and chemical reaction taken together into account. Ahmed *et al.*, [9] investigated the fluids ability to transport heat through an increasingly extending curved surface when there is varying thermal conductivity. Studying the fundamental objective of this investigation is to determine how Williamson fluids travel in heat across an exponentially stretched porous curved surface with a heat source. Mjankwi *et al.*, [10] studied because unstable MHD flocks of nanofluids have been reported to possess varying in terms of both thermal conductivity and fluid characteristics and the temperature change-related diffusion coefficient, across an inclined stretched sheet that is permeable in the heat radiation and chemical response are present. The issue has a significant impact on the cooling technique for the goal of enhancing heated object mechanical characteristics sheet that can't be cooled using conventional techniques based on the fundamentals. Williamson nanofluid MHD boundary layer flow is introduced the effects of the slip parameters, and the velocity power index parameter are investigated throughout an extended sheet with a varying thickness [11]. It is possible to run the bio convection whenever there is non-Newtonian nanofluid to improve thermal efficiency and extrusion mechanisms in a variety of shipment activities [12]. Convergent approach has been used to solve the generated flow problem analytically. Khan *et al.*, [13] investigated Williamson nanofluid with gyrotactic microorganisms and heat radiation under bio convection MHD flow numerical analysis of a new iterative technique. It is numerically examined how radiative and viscous dissipation influence a hydro nanofluid flow with viscous MHD of an upright plate in a study by Lakshmi *et al.*, [14]. Various effects of convective mix Jeffery fluid movement across an extended sheet were studied by Madhavi [15]. Some recent investigations on gyrotactic microorganisms were carried out by many researchers [16-19]. The impact of key parameters on the flow of Casson nanofluid in a liquid thin film over an elongated sheet was investigated by Vijaya *et al.*, [20].

Madhavi and Sravanthi [19] investigated flow of nanofluid in the presence of gyros on a stretched surface subjected to magnetic field and activation energy. The upfront intension of this study is to explore the advances in electrically conducting Casson fluid induced due to a porous elongated surface taking Arrhenius activation energy [21]. In the present paper, the numerical analysis of gyrotactic microorganisms in Williamson nanofluids in the presence of chemical reaction and variable thermal conductivity were investigated.

2. Methodology

The current work considers a two dimensional, steady of numerical analysis of gyrotactic microorganisms in Williamson nanofluids in the presents of chemical and variable thermal conductivity along with porous media. The flow is modelled with the influence of gyrotactic microorganisms and bio convection beneath the influence of radiative flow of heat. In the stretching sheet the Cartesian coordinates x-axis guidance with the velocity $u_w = u_0(x+b)^m$. Since the stretchable sheet surface's normal direction is along the y axis. The surface thickness is a function of $y = A(x+b)^{\frac{1-m}{2}}$, where $A \geq 0$ represents the surface's constant and m is the velocity power index, T_w and C_w are and focus of the wall. T_∞ and C_∞ are ambient temperature and concentration.

Consider the nanofluid that is unaffected by the direction and velocity of swimming microorganisms. Low Reynolds number, B-strength magnetic field was applied in the direction of the y-axis. Figure 1 depicts a flowchart setup. The nonlinear PDEs can be given below in Eq. (1) to Eq. (5).

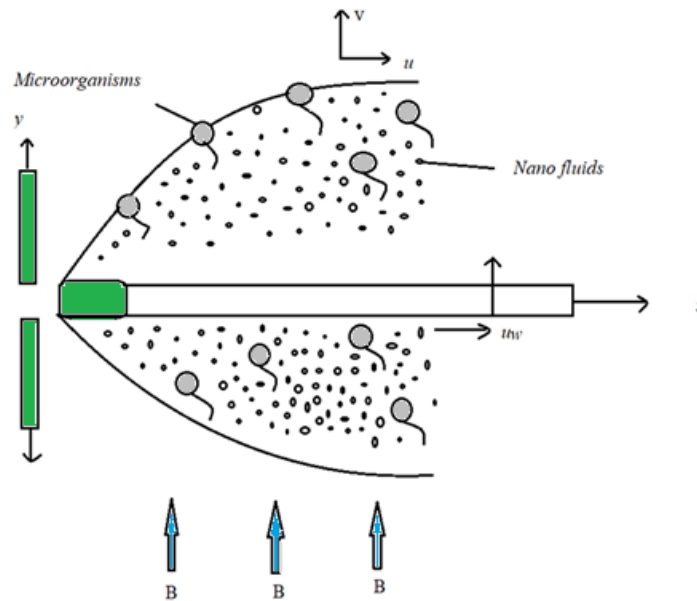


Fig. 1. Geometry of the Problem

$$u \frac{\partial u}{\partial x} + v \frac{\partial u}{\partial y} = 0 \quad (1)$$

$$u \frac{\partial u}{\partial x} + v \frac{\partial u}{\partial y} = \nu \frac{\partial^2 u}{\partial y^2} - \frac{\sigma B_0^2}{\rho} u + 2^{1/2} \nu \Gamma \left(\frac{\partial u}{\partial y} \right) \left(\frac{\partial^2 u}{\partial y^2} \right) - \frac{\nu}{k} u \quad (2)$$

$$u \frac{\partial T}{\partial x} + v \frac{\partial T}{\partial y} = \frac{1}{\rho C_p} \frac{\partial}{\partial y} \left(K(T) \frac{\partial T}{\partial y} \right) - \frac{1}{\rho C_p} \left(\frac{\partial q_r}{\partial y} \right) + \frac{\rho C_p}{\rho C_f} \left(D_B \frac{\partial C}{\partial y} \frac{\partial T}{\partial y} + \frac{D_T}{T_\infty} \left(\frac{\partial T}{\partial y} \right)^2 \right) + \frac{\sigma B_0^2}{\rho_0 C_p} u \quad (3)$$

$$u \frac{\partial C}{\partial x} + v \frac{\partial C}{\partial y} = \frac{D_T}{T_\infty} \left(\frac{\partial^2 T}{\partial y^2} \right) + D_B \left(\frac{\partial^2 C}{\partial y^2} \right) - k(C - C_\infty) \quad (4)$$

$$u \frac{\partial N}{\partial x} + v \frac{\partial N}{\partial y} + \frac{bW_c}{C_w - C_\infty} \left(\frac{\partial N}{\partial y} \frac{\partial C}{\partial y} + N \frac{\partial^2 C}{\partial y^2} \right) = D_m \left(\frac{\partial^2 N}{\partial y^2} \right) \quad (5)$$

In the equations above, the variables ν , D_B , T , C , T_∞ , C_∞ , bW_c , D_m , N stand for, respectively, kinematic viscosity, Brownian diffusion coefficient, temperature and concentration of fluid, ambient temperature and concentration, cell swimming speed, diffusivity of microorganism, and microorganism concentration. Following are the boundary conditions of the surface away from the sheet:

$$u = u_w(x) = U_0(x+b)^m, v = 0, T = T_w, C = C_w, N = N_w, \text{ for } y = (x+b)^{\frac{1-m}{2}} \text{ and} \quad (6)$$

$$u = 0, T = T_\infty, C = C_\infty, N = N_\infty \text{ for } y = \infty$$

The radiation is provided by

$$q_r = -\frac{4\sigma^*}{3k^*} \left(\frac{\partial T^4}{\partial y} \right), \quad (7)$$

By ignoring the higher order of T_∞ and extending the Taylor's series at that temperature T_∞ .

$$T^4 = 4T_\infty^3 T - 3T_\infty^4. \quad (8)$$

Making use of Eq. (7) and Eq. (8), we get

$$\frac{\partial q_r}{\partial y} = -\left(\frac{16\sigma^* T_\infty^3}{3k^*} \right) \left(\frac{\partial^2 T}{\partial y^2} \right). \quad (9)$$

The non-dimensional conditions are defined as below

$$\eta = \sqrt{\frac{U_0(m-1)}{2\nu}} \left(y(x+b)^{\frac{m-1}{2}} - A \right), \quad \psi = \sqrt{\frac{2\nu U_0}{m+1}} (x+b)^{\frac{m+1}{2}} f(\eta), \quad \theta(\eta) = \frac{T - T_\infty}{T_w - T_\infty}, \quad (10)$$

$$\phi(\eta) = \frac{C - C_\infty}{C_w - C_\infty}, \quad G(\eta) = \frac{N - N_\infty}{N_w - N_\infty}.$$

Eq. (1) to Eq. (5) are translated into the following dimensionless non-linear ODEs via similarity transformations (10).

$$f''' + \lambda f''' f'' + ff'' - \left(\frac{2m}{m+1} \right) f'^2 - (M + K_p) f' = 0 \quad (11)$$

$$\left(1 + \epsilon \theta + \frac{4}{3} Rd \right) \theta'' + \epsilon \theta'^2 + \frac{Nc}{Le} \theta' \phi' + \frac{Nc}{Le N_b} \theta'^2 + Pr f \theta' + M Pr Ec f' = 0 \quad (12)$$

$$\phi'' + Le Pr f \phi' + \frac{1}{N_b} \theta'' - K_r \phi = 0 \quad (13)$$

$$G'' + 2\sqrt{\frac{m+1}{m-1}} Sc f G' - Pe (\phi' G' + (\Omega + G) \phi'') = 0 \quad (14)$$

The boundary conditions are given below

$$f'(0) = 1, f(0) = \alpha \left(\frac{1-m}{1+m} \right), \quad \theta(0)=1, \phi(0) = 1, G(0) = 1 \text{ at } \eta=0, \text{ and} \quad (15)$$

$$f'(\infty) = 0, \theta(\infty)=0, \phi(\infty) = 0, G(\infty) = 0, \text{ at } \eta=\infty$$

Dimensionless coordinates of technical interest like skin friction, Nusselt and Sherwood numbers and regional density index of motile microbes may be defined as

$$\text{Re}_x^{1/2} C f_x = f''(0), \text{Nu}_x \text{Re}_x^{-1/2} = -\theta'(0), \text{Sh}_x \text{Re}_x^{-1/2} = -\phi'(0), \text{Nn}_x \text{Re}_x^{-1/2} = -G'(0), \quad (16)$$

Determining the parameters in the following equation.

where

$$\Omega = \frac{N_\infty}{N_w - N_\infty}, \text{Le} = \frac{\alpha}{D_B}, \text{Pe} = \frac{bW_c}{D_m}, \text{Ec} = \frac{U_0^2}{c_p(T_w - T_\infty)}, N_b = \frac{BT_\infty(C_w - C_\infty)}{DT(T_w - T_\infty)}, N_c = \frac{\rho_p c_p(C_w - C_\infty)}{\rho_c}, \text{Rd} = \frac{4\sigma^* T_\infty^3}{k^* k_\infty}, \text{Pr} = \frac{\nu}{\alpha},$$

$$\text{Sc} = \frac{\nu}{D_B}, K_p = \frac{\nu x}{k u_e}, M = \frac{\sigma B_0^2 x}{\rho U_0(1+m)}, \delta = \frac{T_w - T_\infty}{T_\infty}, K_r = \frac{K}{\rho c_p} (T_w - T_\infty), \lambda = T \sqrt{\frac{U_0^3(x+b)^{3m-1}(m+1)}{\nu}}. \quad (17)$$

2.1 Numerical Solutions

Employing the boundary layer theory, The PDEs (1) to (5) are changed into nonlinear coupled ODEs. By using boundary conditions (15), these closely related ODEs (11) to (14) are numerically solved using MATLAB's renowned BVP4C solver. The three-stage Lobatto IIIa collocation algorithm used by the BVP4C solver yields a C1 continuous solution that is 4th-order accurate over the whole domain.

2.2 Runge-Kutta Method

The Runge-kutta method is applied before that, first apply the PDEs into ODEs of first order. Let us consider $x_1 = \eta, x_2 = f, x_3 = f', x_4 = f'', x_5 = \theta, x_6 = \theta', x_7 = \phi, x_8 = \phi', x_9 = G, x_{10} = G'$. Following system is obtained.

$$\begin{pmatrix} x_1' \\ x_2' \\ x_3' \\ x_4' \\ x_5' \\ x_6' \\ x_7' \\ x_8' \\ x_9' \\ x_{10}' \end{pmatrix} = \begin{pmatrix} 1 \\ x_3 \\ x_4 \\ \frac{1}{1+\lambda x_4} \left(\frac{2m}{m+1} x_3^2 + (M + Kp)x_3 - x_2 x_4 \right) \\ x_6 \\ \frac{1}{1+\epsilon x_5 + \frac{4}{3} \text{Rd}} \left(-\text{Pr} x_2 x_6 - \frac{N_c}{\text{Le}} x_6 x_8 - \epsilon x_6^2 - \frac{N_c}{\text{Le} N_b} x_6^2 - M \text{Pr} E_c x_3 \right) \\ x_8 \\ -\frac{1}{N_b} x_6' - \text{Le} \text{Pr} x_2 x_8 + K_r x_7 \\ x_{10} \\ -\text{Sc} \sqrt{\frac{(m+1)}{m-1}} x_2 x_{10} + \text{Pe} (x_8 x_{10} + (x_8' (x_9 + \Omega))) \end{pmatrix} \quad (18)$$

The boundary conditions are

$$\begin{pmatrix} x_1 \\ x_2 \\ x_3 \\ x_4 \\ x_5 \\ x_6 \\ x_7 \\ x_8 \\ x_9 \\ x_{10} \end{pmatrix} = \begin{pmatrix} 1 \\ \alpha \left(\frac{1-m}{1+m} \right) \\ 1 \\ u_1 \\ 1 \\ u_2 \\ 1 \\ u_3 \\ 1 \\ u_4 \end{pmatrix} \quad (19)$$

By using Runge-Kutta method Eq. (18) and Eq. (19) are solved. Appropriate initial circumstances u_1, u_2, u_3 and u_4 are estimated using the Newton's technique until the boundary conditions at $f(\infty) = 1, \vartheta(\infty)=0, \varnothing(\infty)=0, G(\infty)=0$.

3. Results and Discussion

In the present paper the velocity, temperature, concentration and density of microorganism concentration profiles are changes from Figure 2 to Figure 23. $A=0.1, m=2, Pe=2, B=1, Rd=2, Nc=0.1, M=2, Sc=0.1, Kr=0.1, Le=1, C=0.1, K=0.1, Nb = 4, Kp = 2, Ec=0.1, Pr=3.5$. In Figure 2 and Figure 3, the values of magnetic field parameter increase, the velocity profiles decrease, and temperature profiles increase. Because the magnetic field produces Lorentz forces, the Lorentz force causes an increase in fluid viscosity.

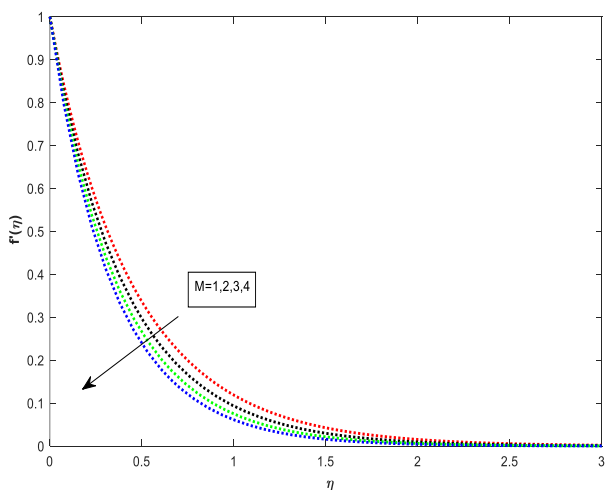


Fig. 2. $f'(\eta)$ for several variations in M

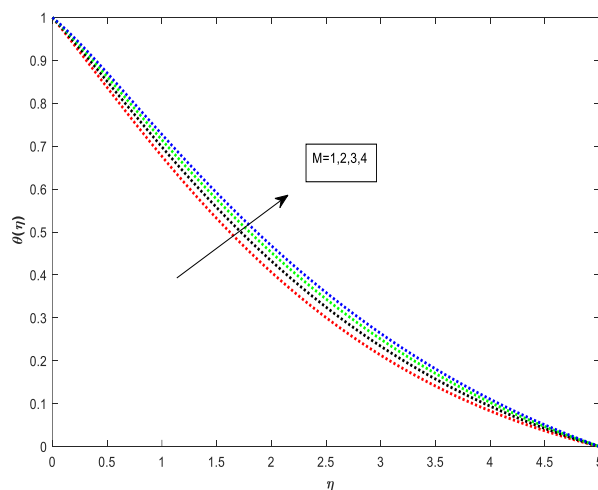


Fig. 3. $\theta(\eta)$ for several variations in M

The temperature and velocity profiles are shifting downward and upward as a result of increasing the parameter Kp . It seems in Figure 4 and Figure 5.

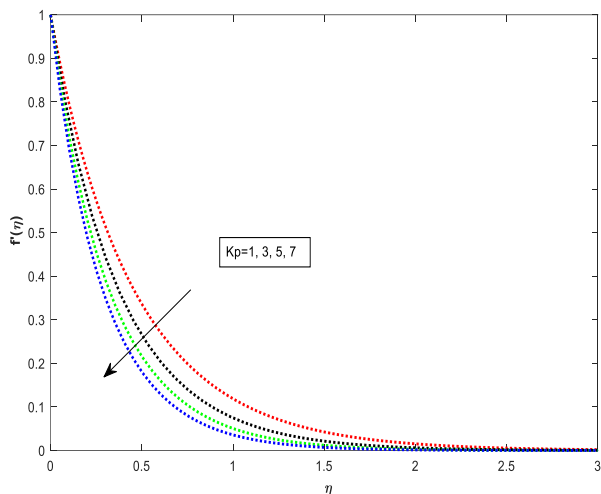


Fig. 4. $f'(\eta)$ for several variations in K_p

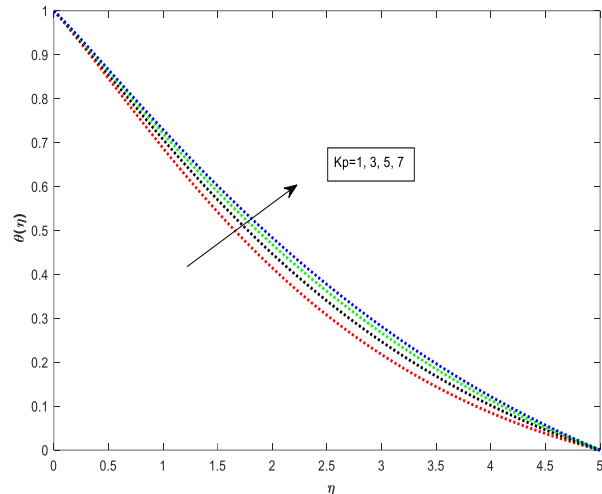


Fig. 5. $\theta(\eta)$ for several variations in K_p

Figure 6 and Figure 7 illustrate Williamson parameter increases the velocity profiles are decreases temperature profiles are increasing. The viscoelastic shear thinning property of non-Newtonian fluid is present in the Williamson parameter.

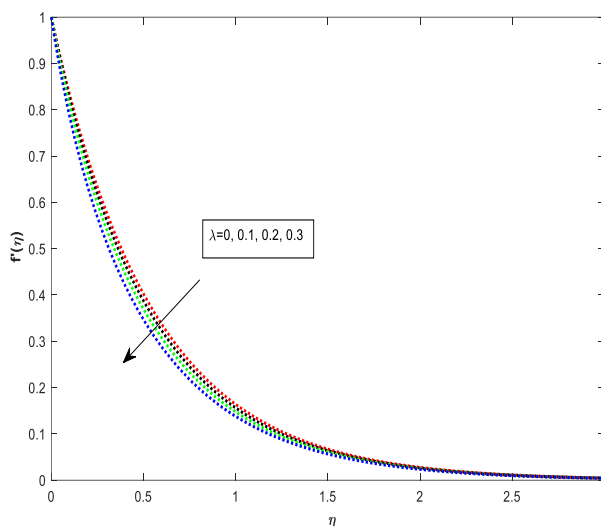


Fig. 6. $f'(\eta)$ for several variations in λ

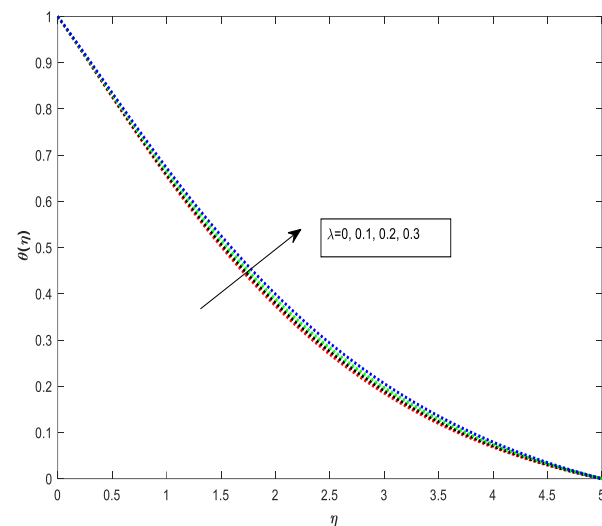


Fig. 7. $\theta(\eta)$ for several variations in λ

Figure 8 to Figure 10 represent Prandtl number Pr rises temperature, concentration and density of microorganism concentration profiles decrease. According to the definition of Pr , the temperature profile is decreased by decreasing the fluid's thermal conductivity when the Prandtl number is escalates. Furthermore, thermal boundary layer thickness declines with increasing Prandtl number Pr . As a result, heat transfers quickly, which lowers the temperature of the substance.

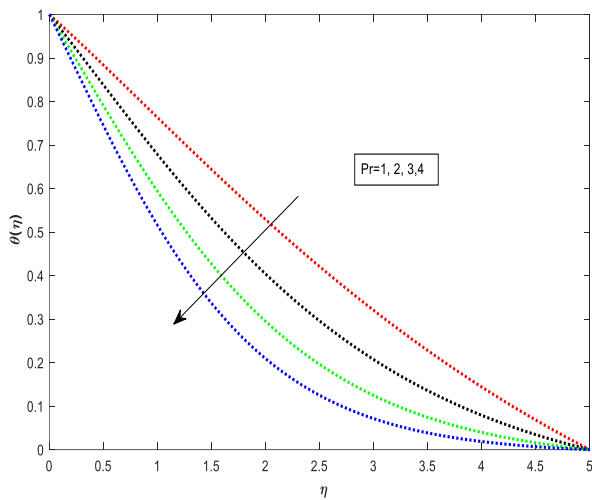


Fig. 8. $\theta(\eta)$ for several variations in P_r

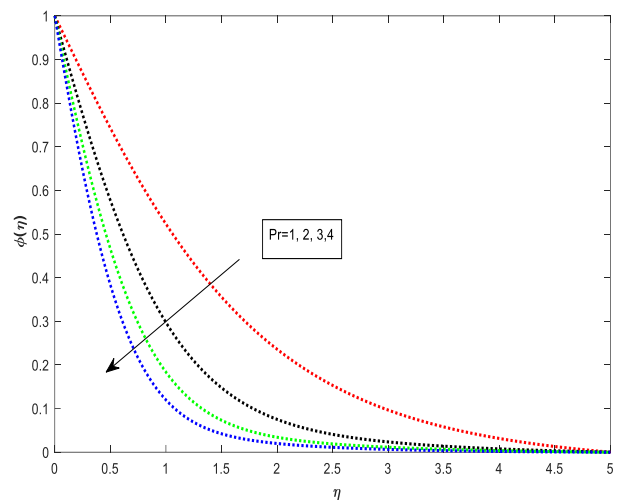


Fig. 9. $\phi(\eta)$ for several variations in P_r

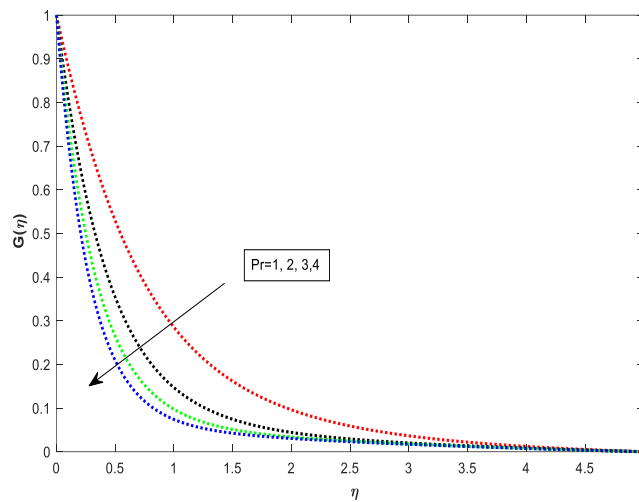


Fig. 10. $G(\eta)$ for several variations in P_r

The effect of Brownian diffusivity and Lewis number on temperature, concentration and microorganisms' concentration profiles are plotted in Figure 11 to Figure 13 and Figure 14 to Figure 16 respectively. The parameters N_b and Le increases the temperature, concentration and microorganisms' concentration profiles are diminishes. Since N_b represents of a Particle is the thermal motion of the molecular agitation of the liquid medium, size of nanoparticles and Brownian motion are connected, in diffusion the particle moves in the direction of high concentration to low concentration, a rise in N_b indicates an increase in the activity of the nanofluid particles. Since Le is the proportion of thermal to Brownian diffusion, it is physically impossible for Le to be equal to zero. With an increase in N_b , Thermal boundary layer and temperature profile degradation has been observed. Temperature profiles only exhibit very slight fluctuation when thermophoretic diffusivity is very small in comparison to Brownian diffusivity.

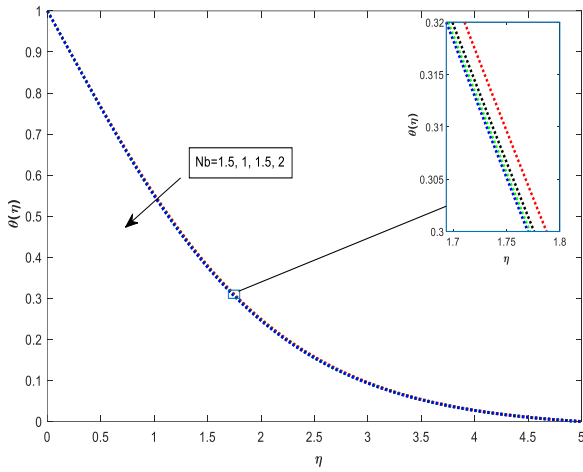


Fig. 11. $\theta(\eta)$ for several variations in N_b

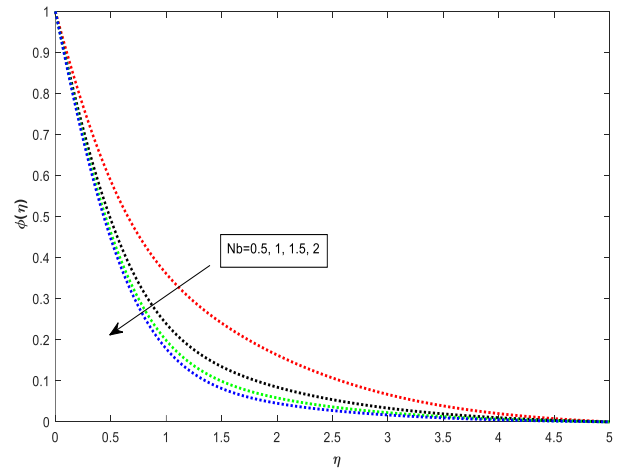


Fig. 12. $\phi(\eta)$ for several variations in N_b

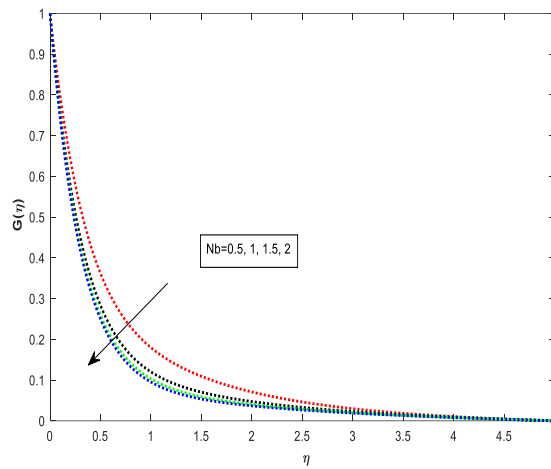


Fig. 13. $G(\eta)$ for several variations in N_b

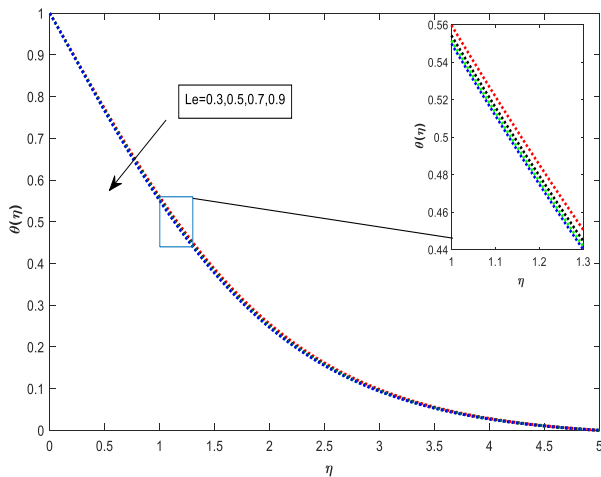


Fig. 14. $\theta(\eta)$ for several variations in Le

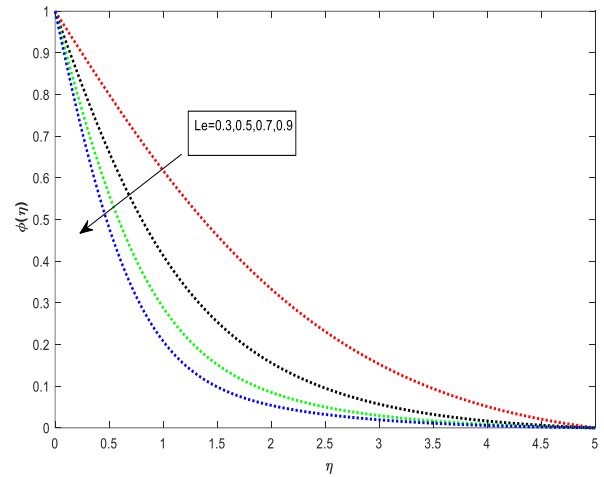


Fig. 15. $\phi(\eta)$ for several variations in Le

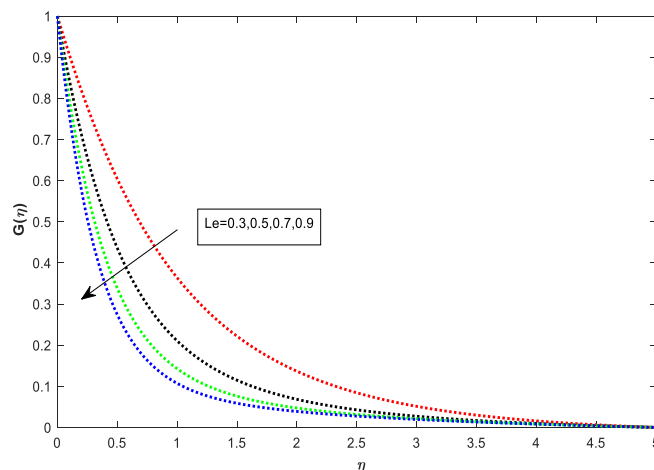


Fig. 16. $G(\eta)$ for several variations in Le

In Figure 17 temperature profiles are increases when radiation parameter increases because of the changing radiation parameter, the mean absorption efficiency declines, raising the fluid's temperature. The effect of the Eckert number is displayed in Figure 18.

From the graph, it can be seen that the distribution of heat increases as the Eckert number rises. The ratio of boundaries layer enthalpy to the kinetic energy is known as the Eckert factor. Therefore, increasing the Eckert number's value results in an increase the value of the heat distribution.

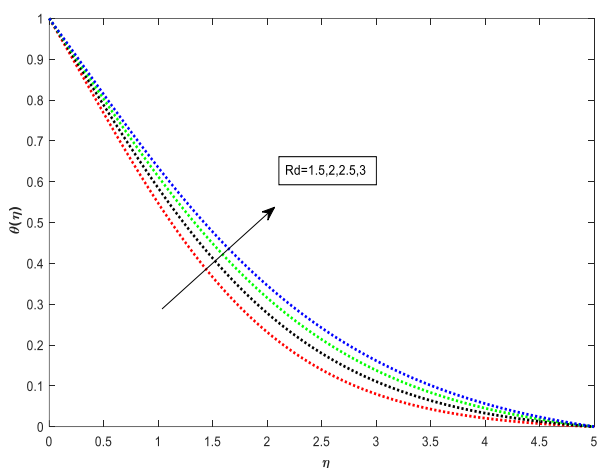


Fig. 17. $\theta(\eta)$ for several variations in R_d

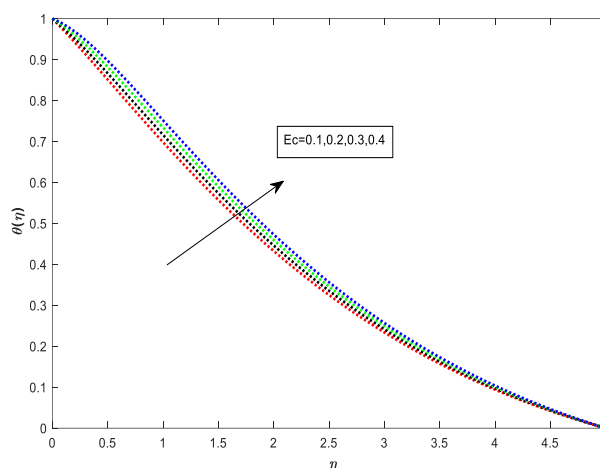


Fig. 18. $\theta(\eta)$ for several variations in Ec

Figure 19 and Figure 20 demonstrate the relevance and impact of variable thermal conductivity constant ϵ on the temperature profile $\theta(\eta)$ concentration profile $\phi(\eta)$, as increase ϵ , the temperature profile also increases. While nanoparticle volume fraction profiles show the opposite phenomenon. As a result, the premise that thermal conductivity changes with temperature predicts that the transverse velocity $\frac{\partial}{\partial y} \left(K \frac{\partial T}{\partial y} \right)$ in Eq. (3) will be reduced by a certain amount. When using a coolant material with a low thermal conductivity characteristic, cooling happens significantly more quickly.

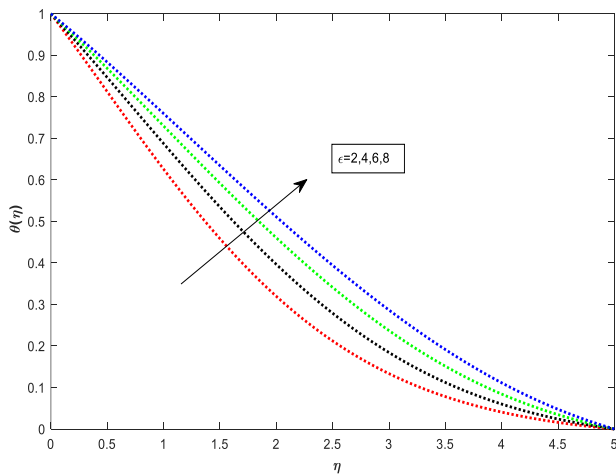


Fig. 19. $\theta(\eta)$ for several variations in ϵ

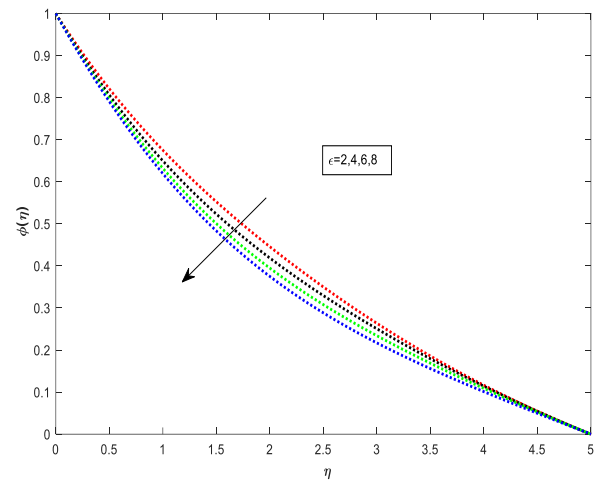


Fig. 20. $\phi(\eta)$ for several variations in ϵ

Figure 21 shows that as K_r grows, the concentration profile drops, which indicates that K_r is sluggish agent because it lowers the concentration in the boundary layer, causing the solute boundary layer to become thinner and accelerate mass transfer at the site immediately adjacent to the sheet.

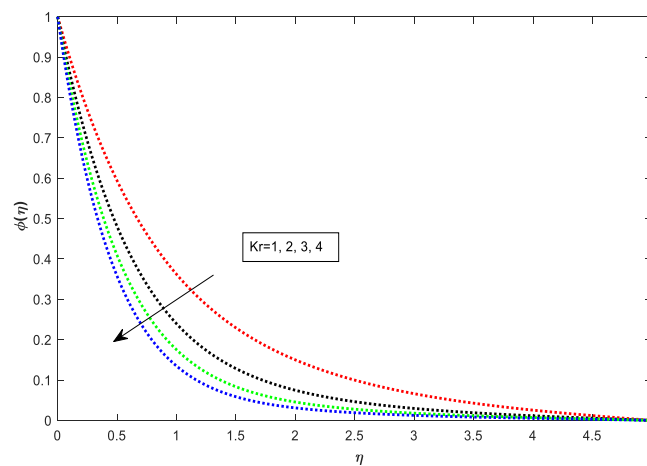


Fig. 21. $\phi(\eta)$ for several variations in K_r

Figure 22 demonstrates that as the Peclet number increases, the density of the profiles of microbe concentrations decreases. Bio convection is caused by microorganisms that are swimming up the fluid's upper surface. An upsurge in the Peclet number Pe , the maximal swimming speed of microbes and their rate of diffusion during their swimming continuum. The fluid's bio convection Peclet number determines the speed of swimming motile microorganisms, which slows them down as they approach the outside due to their thickness. Schmidt number's impact on the bio convection of moving organisms is shown in Figure 23. A declining concentration profile is associated with rising Schmidt number Sc values. As the rate of viscous diffusion increases, the density of motile microorganism's decreases.

Table 1 takes into account the relatively slight variations in the articles between the base study and the current paper. In this article, the disparities in Prandtl numbers are compared.

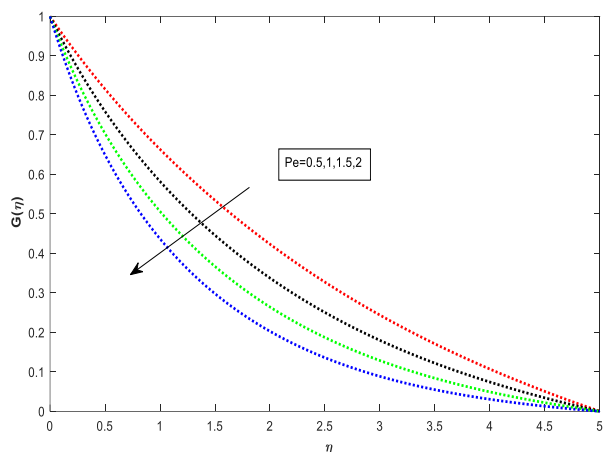


Fig. 22. $G(\eta)$ for several variations in Pe

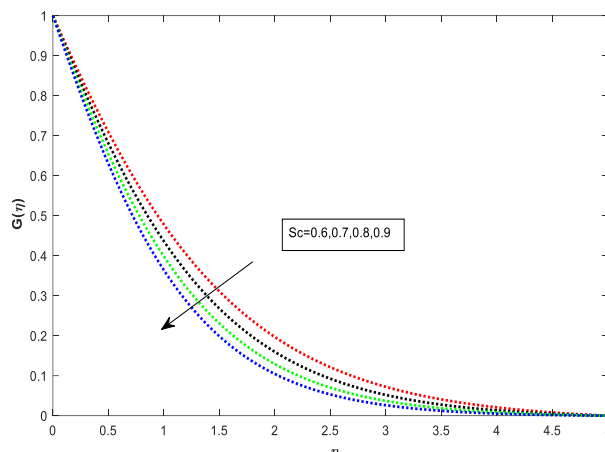


Fig. 23. $G(\eta)$ for several variations in Sc

Table 1

Contrast of $-\theta'(0)$ for different P_r with $K_p = Ec = Kr = 0$

P_r	Khan <i>et al.</i> , [13]	Present result
1	0.258898	0.222143
2	0.349549	0.314989
3	0.451902	0.412214
4	0.562480	0.507621

In Table 2 and Table 3, it is described that the variations of skin friction, Nusslet, Sherwood number and local density number of motile microorganism for various parameters. i.e., M , K_p , λ , Pr , N_b , Le , Rd , Ec , ϵ , Kr , Pe and Sc .

Table 2

Re_x , Nu_x , Sh_x and Nn_x variations for different parameters

M	K_p	λ	Pr	N_b	Le	$Re_x^{1/2} C_f$	$Nu_x Re_x^{-1/2}$	$shRe_x^{-1/2}$	$NnRe_x^{-1/2}$
1						2.286815	0.312306	0.379785	0.907986
2						2.566011	0.271859	0.393229	0.934268
3						2.825985	0.238543	0.404634	0.956787
4						3.071794	0.210184	0.414574	0.976567
	1					2.286815	0.281480	0.394455	0.939978
	3					2.825985	0.264322	0.392270	0.929764
	5					3.306749	0.253167	0.390780	0.922850
	7					3.753339	0.245206	0.389621	0.917628
		0				1.844311	0.333624	0.379734	0.272481
		1				1.980130	0.329058	0.379761	0.271470
		2				2.193972	0.323563	0.379798	0.270261
		3				2.754924	0.316073	0.379847	0.268626
			1			1.200110	0.222143	0.525858	1.239328
			2			1.200110	0.314989	0.931992	2.119127
			3			1.200110	0.412214	1.252360	2.817043
			4			1.200111	0.507621	1.530503	3.424595
				0.5		1.200109	0.461744	0.996447	2.261874
				1.0		1.200111	0.460973	1.224938	2.758308
				1.5		1.200110	0.460716	1.300794	2.923353
				2.0		1.200109	0.460588	1.300794	3.005792
					0.3	1.200110	0.453963	0.404348	0.978286
					0.5	1.200109	0.461112	0.729863	1.680885
					0.7	1.200109	0.465161	0.996706	2.260373
					0.9	1.200109	0.467756	1.228656	2.765724

Table 3
 Re_x, Nu_x, Sh_x and Nn_x variations for different parameters

Rd	Ec	€	Kr	Pe	Sc	$Re_x^{1/2} C_f$	$Nu_x Re_x^{-1/2}$	$shRe_x^{-1/2}$	$NnRe_x^{-1/2}$
1.5						1.200110	0.449521	0.357420	0.285303
2.0						1.200110	0.413582	0.372868	0.286822
2.5						1.200110	0.385813	0.384888	0.287997
3.0						1.200110	0.363942	0.394408	0.288922
	0.1					2.566011	0.271859	0.393229	0.934268
	0.2					2.566011	0.215903	0.419979	0.992677
	0.3					2.566011	0.159931	0.446739	1.051117
	0.4					2.566011	0.103944	0.473511	1.109587
		2				1.200110	0.360728	0.396241	0.289214
		4				1.200110	0.292616	0.425988	0.292186
		6				1.200110	0.250457	0.444393	0.293964
		8				1.200110	0.221978	0.456998	0.295144
			1			1.200110	0.391828	1.053572	2.387594
			2			1.200110	0.385009	1.473894	3.304646
			3			1.200110	0.381587	1.793517	4.003621
			4			1.200110	0.379440	2.061942	4.591345
				0.5		1.200110	0.413582	0.372868	0.407211
				1.0		1.200110	0.413582	0.372868	0.567479
				1.5		1.200110	0.413582	0.372868	0.736736
				2.0		1.200110	0.413582	0.372868	0.913111
					0.6	1.200110	0.413582	0.372868	0.623809
					0.7	1.200110	0.413582	0.372868	0.689092
					0.8	1.200110	0.413582	0.372868	0.752225
					0.9	1.200110	0.413582	0.372868	0.813163

4. Conclusions

In the present paper numerical analysis of gyrotactic microorganisms in Williamson nanofluids with chemical reaction and variable thermal conductivity is observed. The PDEs converted into ODEs by using similarity transformations, RK Fehlberg technique is applied for this. A few crucial conclusions are given below.

- i. The Magnetic field, Permeability and Williamson parameters are upgrade the velocity and temperature profiles are decline and raising respectively.
- ii. The prandtl number, Brownian diffusion and Lewis numbers are increase the velocity, temperature and concentration profiles are decreasing.
- iii. The Parameters Rd, Ec and € raises the temperature profiles are escalating.
- iv. The variable thermal conductivity constant €, Kr and Sc, Pe are escalating the concentration and concentration of motile microorganism's profiles are decelerates.

References

- [1] Choi, S. U. S, and Jeffrey A. Eastman. *Enhancing thermal conductivity of fluids with nanoparticles*. No. ANL/MSD/CP-84938; CONF-951135-29. Argonne National Lab.(ANL), Argonne, IL (United States), 1995.
- [2] Khan, M. Waleed Ahmed, M. Ijaz Khan, T. Hayat, and A. Alsaedi. "Entropy generation minimization (EGM) of nanofluid flow by a thin moving needle with nonlinear thermal radiation." *Physica B: Condensed Matter* 534 (2018): 113-119. <https://doi.org/10.1016/j.physb.2018.01.023>
- [3] Nield, D. A., and A. V. Kuznetsov. "The Cheng-Minkowycz problem for natural convective boundary-layer flow in a porous medium saturated by a nanofluid." *International Journal of Heat and Mass Transfer* 52, no. 25-26 (2009): 5792-5795. <https://doi.org/10.1016/j.ijheatmasstransfer.2009.07.024>

- [4] Kuznetsov, A. V. "The onset of nanofluid bioconvection in a suspension containing both nanoparticles and gyrotactic microorganisms." *International Communications in Heat and Mass Transfer* 37, no. 10 (2010): 1421-1425. <https://doi.org/10.1016/j.icheatmasstransfer.2010.08.015>
- [5] Kuznetsov, Andrey V. "Nanofluid bioconvection in water-based suspensions containing nanoparticles and oxytactic microorganisms: oscillatory instability." *Nanoscale Research Letters* 6 (2011): 1-13. <https://doi.org/10.1186/1556-276X-6-100>
- [6] Mallikarjuna, B., A. M. Rashad, Ali Chamkha, and M. M. M. Abdou. "Mixed bioconvection flow of a nanofluid containing gyrotactic microorganisms past a vertical slender cylinder." *Frontiers in Heat and Mass Transfer (FHMT)* 10 (2018). <https://doi.org/10.5098/hmt.10.21>
- [7] Uddin, Mohammed Jashim, Yasser Alginahi, O. Anwar Bég, and Muhammad Nomani Kabir. "Numerical solutions for gyrotactic bioconvection in nanofluid-saturated porous media with Stefan blowing and multiple slip effects." *Computers & Mathematics with Applications* 72, no. 10 (2016): 2562-2581. <https://doi.org/10.1016/j.camwa.2016.09.018>
- [8] Shahid, A., Z. Zhou, M. M. Bhatti, and D. Tripathi. "Magnetohydrodynamics nanofluid flow containing gyrotactic microorganisms propagating over a stretching surface by successive Taylor series linearization method." *Microgravity Science and Technology* 30 (2018): 445-455. <https://doi.org/10.1007/s12217-018-9600-2>
- [9] Ahmed, Kamran, Waqar A. Khan, Tanvir Akbar, Ghulam Rasool, Sayer O. Alharbi, and Ilyas Khan. "Numerical investigation of mixed convective Williamson fluid flow over an exponentially stretching permeable curved surface." *Fluids* 6, no. 7 (2021): 260. <https://doi.org/10.3390/fluids6070260>
- [10] Mjankwi, Musa Antidius, Verdiana Grace Masanja, Eunice W. Mureithi, and Makungu Ng'oga James. "Unsteady MHD flow of nanofluid with variable properties over a stretching sheet in the presence of thermal radiation and chemical reaction." *International Journal of Mathematics and Mathematical Sciences* 2019 (2019). <https://doi.org/10.1155/2019/7392459>
- [11] Razi, Shazwani Md, Siti Khuzaimah Soid, Ahmad Sukri Abd Aziz, Noorashikin Adli, and Zailaha Md Ali. "Williamson nanofluid flow over a stretching sheet with varied wall thickness and slip effects." In *Journal of Physics: Conference Series*, vol. 1366, no. 1, p. 012007. IOP Publishing, 2019. <https://doi.org/10.1088/1742-6596/1366/1/012007>
- [12] Khan, Sami Ullah, Sabir Ali Shehzad, and Nasir Ali. "Bioconvection flow of magnetized Williamson nanofluid with motile organisms and variable thermal conductivity." *Applied Nanoscience* 10 (2020): 3325-3336. <https://doi.org/10.1007/s13204-020-01282-5>
- [13] Khan, Muhammad Jebran, Samina Zuhra, Rashid Nawaz, Balaganesh Duraisamy, Mohammed S. Alqahtani, Kottakaran Soopy Nisar, Wasim Jamshed, and Mohamed Abbas. "Numerical analysis of bioconvection-MHD flow of Williamson nanofluid with gyrotactic microbes and thermal radiation: New iterative method." *Open Physics* 20, no. 1 (2022): 470-483. <https://doi.org/10.1515/phys-2022-0036>
- [14] Lakshmi, G. Vijaya, G. Raghavendra Ganesh, W. Sridhar, and M. Radha Madhavi. "MHD hydro-nanofluid flow over upright plate in presence of radiation and viscous dissipation." In *AIP Conference Proceedings*, vol. 2375, no. 1. AIP Publishing, 2021. <https://doi.org/10.1063/5.0066411>
- [15] Madhavi, M. Radha. "Impacts of Thermophoresis, Joule heating and Soret & Dufour effects on mixed convective Jeffery fluid flow over an elongated sheet." *International Journal of Advanced Science and Technology* 29, no. 5 (2020): 3060-3069.
- [16] Reddy, C. Srinivas, Farhan Ali, Khaled Al-Farhany, and W. Sridhar. "Numerical analysis of gyrotactic microorganisms in MHD radiative Eyring-Powell nanofluid across a static/moving wedge with Soret and Dufour effects." *ZAMM-Journal of Applied Mathematics and Mechanics/Zeitschrift für Angewandte Mathematik und Mechanik* 102, no. 11 (2022): e202100459. <https://doi.org/10.1002/zamm.202100459>
- [17] Sharafatmandjoo, Shervin, and C. S. Nor Azwadi. "Effect of Imposition of viscous and thermal forces on Dynamical Features of Swimming of a Microorganism in nanofluids." *Journal of Advanced Research in Micro and Nano Engineering* 8, no. 1 (2022): 1-8.
- [18] Sridhar, Wuriti, Garishe Vijaya Lakshmi, Khaled Al-Farhany, and Ganugapati Raghavendra Ganesh. "MHD Williamson nanofluid across a permeable medium past an extended sheet with constant and irregular thickness." *Heat Transfer* 50, no. 8 (2021): 8134-8154. <https://doi.org/10.1002/htj.22270>
- [19] Madhavi, M., and P. Sravanthi. "Nanofluid Flow in Presence of Gyrotactic Microorganisms on the Stretching Surface With Magnetic Field and Activation Energy." *Frontiers in Heat and Mass Transfer (FHMT)* 19 (2022). <https://doi.org/10.5098/hmt.19.40>
- [20] Vijaya, N., Sunil Babu G., and Vellanki Lakshmi N. "Influence of critical parameters on liquid thin film flow of casson nano fluid over elongated sheet under thermophoresis and brownian motion." *Frontiers in Heat and Mass Transfer (FHMT)* 15, no. 1 (2020). <https://doi.org/10.5098/hmt.15.23>

- [21] Nagalakshmi, P. S. S., N. Vijaya, and Shaik Mohammed Ibrahim. "Entropy Generation of Three-Dimensional Williamson Nanofluid Flow Explored with Hybrid Carbon Nanotubes over a Stretching Sheet." *CFD Letters* 15, no. 7 (2023): 112-130. <https://doi.org/10.37934/cfdl.15.7.112130>